

Veröffentlichung

Im Rahmen des SFB 880. www.sfb880.tu-braunschweig.de

Autoren

Savoni, Luciana ;Rudnik, Ralf

Titel

Aerodynamic Assessment of Pylon-Mounted Over-the-Wing Engine Installations on a STOL Commercial Aircraft Concept

Publisher o. Konferenz

New Results in Numerical and Experimental Fluid Mechanics, Vol. 11, pp 51-60, Springer Verlag, ed. A. Dillmann, et.al.

Jahr

2016

Internet-Link (Doi-Nr.)

Aerodynamic Assessment of Pylon-Mounted Over-the-Wing Engine Installations on a STOL Commercial Aircraft Concept

Luciana Savoni, Ralf Rudnik

Abstract Aerodynamic interference effects and potential benefits of an over-the-wing mounted (OWM) engine installation are examined with CFD methods. The reference configuration is a novel transport aircraft concept with STOL capabilities. The wing/body configuration is compared to the wing/body/engine configuration with power-off nacelle. Subsequently, jet-on computations are carried out to address the influence of the jet presence on the engine/airframe interference effects. The engine is initially considered in a reference position. Successively, position variations of the engine are performed to analyze the interaction with the supersonic region and shocks on the wing upper surface. To conclude the study, a preliminary evaluation of the installation drag is done, to investigate the potential of favorable interference effects and reduced drag with respect to more conventional under-the-wing mounted (UWM) engines installations.

1 Introduction

Low noise characteristics, low fuel consumption and emissions, and consequently low environmental pollution are some of the most compelling requirements of an aviation technology which is striving to become every day more “environmental friendly”. These requirements can, however, be in net contrast with the growing need of increasing the number of passengers and flights. As shown in [1], the worldwide passenger traffic, measured in Revenue Passenger Kilometers (RPK), is expected to double in the next fifteen years and it will grow by 145% to 15.2 trillion RPKs by 2034. In this scenario, it is quite appealing to incorporate airports which are at present not accessible due to their limited runway size or because of their proximity to residential areas. In a synergistic effort between the German Aerospace Center and the Technical Universities of Braunschweig and Hannover, the Collaborative Research Center (Sonderforschungsbereich) SFB 880 aims to address this need by investigating short take-off and landing (STOL) vehicles with a capability of 100 passengers that feature low noise emissions characteristics. As determined in [2], the capability of taking-off and landing on 800 m runways

L. Savoni · R. Rudnik
DLR, Institute of Aerodynamics and Flow Technology, Lilienthalplatz 7, 38108
Braunschweig, Germany
e-mail: {luciana.savoni, ralf.rudnik}@dlr.de

would double the potential point to point connections with respect to the current situation.

Figure 1 depicts one of the two reference configurations of the SFB 880 [3]. The so-called REF3 configuration is characterized by a low wing mounting allowing the installation of an Ultra High Bypass Ratio (UHBR) turbofan over the wing aft of the trailing edge. This design has proven to offer a considerable potential for an aerodynamically efficient engine installation, a significant noise reduction, a reduced undercarriage length and a decreased risk of foreign object damage during ground operations [4]. Nevertheless, the engine's installation over the wing poses many challenges, especially to manage the interference drag at transonic conditions. Combining this with low noise STOL capabilities represents a new challenge.



Fig. 1 REF3 configuration for SFB 880 with over-the-wing mounted engines.

The present study aims to provide the results of a first investigation about the effects of the installation of an UHBR turbofan engine over the wing, in terms of wing and nacelle interference and a drag assessment in the transonic regime. The engine will be considered in an initial reference position. Subsequently two variations of the vertical position of the engine will be analyzed. More specifically, the engine will be shifted firstly closer to the wing's surface and then further away. The three configurations with the installed engine will be compared to the wing/body (WB) geometry in order to investigate the impact of the engine on the transonic flow phenomena taking place on the wing's upper surface. Finally, some preliminary drag considerations for the three installed configurations will be discussed.

2 Geometry and numerical approach

To evaluate the aerodynamic performance of an over-the-wing mounted engine aircraft, the REF3 wing/body/engine (WBE) configuration has been studied. REF3 configuration features a low wing, pylon integrated landing gears, and a T-tail. The tail is not considered while the engine is placed at the reference position as prescribed by the overall design activity [3]. To be able to separate aerodynamic installation effects, the pylon is omitted. The engine is mounted aft of the wing

trailing edge, because this proved to be beneficial for drag reduction in previous studies [4].

The CENTAUR software [5] has been used to generate the computational grids. Due to the expected increasing complexity of the geometry, a hybrid kind of grid seems to be the most convenient choice. Hybrid grids consist predominantly of prisms and tetrahedras combining the advantages of both, structured and unstructured grids [6]. Structured hexahedras were used to discretize the trailing edges, only.

First, a grid for the WB configuration has been generated featuring about 9 million nodes. 38 prisms layers are used for the near-wall structured region of the grid. The non-dimensional first wall spacing amounts to $y^+ \sim 1$. The WB grid has been used as a starting point to create the WBE mesh. The WBE grid has been generated using CAD and geometric sources in the most crucial regions. The final WBE configurations grids have around 13 million nodes. An example of a WBE grid for the engine in the spanwise reference position $\eta=0.31$ is depicted in Figure 2.

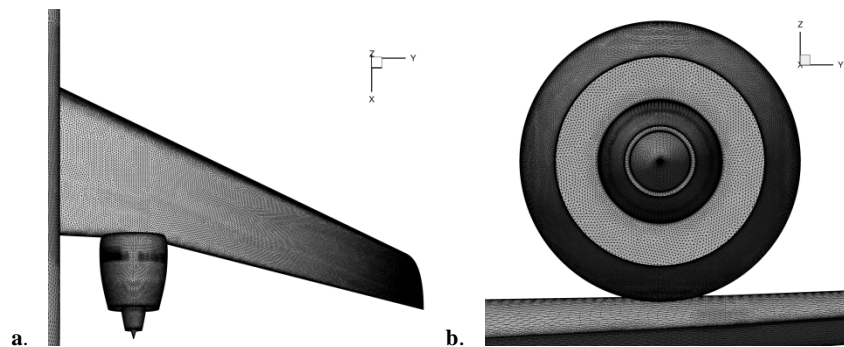


Fig. 2. a. View on the grid of the WBE configuration **b.** Grid detail on the engine.

The simulations have been carried out with the DLR TAU-Code using a finite volume method to solve the 3D RANS equations. The flow solver was used in a cell-centered mode and the spatial discretization was completed employing a central scheme with 80% of artificial matrix dissipation to more accurately describe the transonic flow features such as shock waves.

For the time integration, an implicit (Backward-Euler) algorithm combined with the Lower-Upper Symmetric Gauss-Seidel (LUSGS) scheme described in [6] and [7] is used. Turbulence model is accomplished based on the Spalart-Allmaras in its negative formulation [7].

3 Test case and engine placement

Since the aim of this phase of the studies is the estimation of the aerodynamic performance of OWM engine configurations in high speed, the start of cruise test case has been analyzed. The design conditions related to the test case are summarized in Table 1.

Variable	Value
C_L	0.46
Mach number	0.78
Speed	230.154 m/s
Altitude	11277 m

Table 1. Summary of the considered test case data.

The WB configuration was computed and used as a reference for the interference studies.

The WBE configuration was considered first with the engine in the reference spanwise position $\eta=0.31$. The vertical distance between engine and wing surface was defined through the distance Z between the engine axis and the X axis of the main reference system located at the aircraft nose, as can be seen in [3]. The reference vertical position for the engine corresponds to $Z_{ref}=376$ mm. This case was computed both with jet off and jet on, in order to evaluate the influence of the jet on the flow passing over the wing. Previous studies [4] have proven that the aerodynamic benefit of OW nacelle installations depends on the interaction of the slower inlet/outlet flow with the high speed wing flow field. Finally, two variations of the vertical position of the engine were performed. The engine was placed at $Z_1=0.5*Z_{ref}=188$ mm and at $Z_2=1.5*Z_{ref}=564$ mm. The position variation is depicted in Figure 3. All the simulations were run at constant $C_L=0.46$.

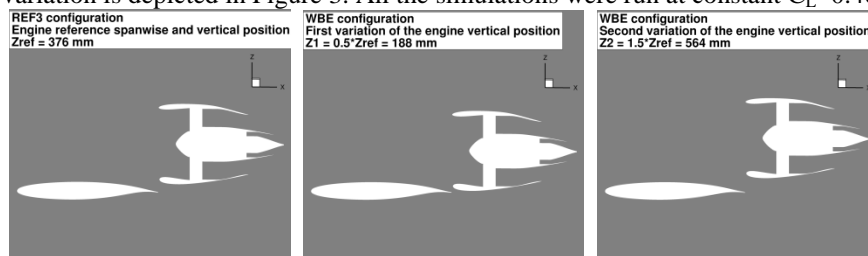


Fig. 3. Vertical variation of the position of the engine (cut at the engine middle plane).

4 Results

In this chapter the results of this preliminary study of the interference effect will be discussed. The computation of the WB configuration is essential in order to allow a first assessment of the extent of the transonic region on the upper wing surface and of the strength and location of the shock. The WB computation reveals a distinct shock at about 75% local chord on most of the wing's upper surface as can be seen in the isobars (Figure 4a) and the pressure distribution at 31% half span (Figure 4b). The mitigation of the shock-related wave drag is the fundamental approach to yield a positive effect of the engine installation on the overall drag [4].

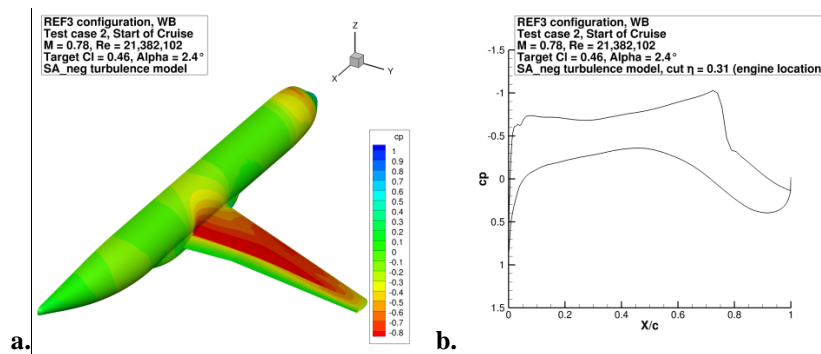


Fig. 4. a. Pressure distribution on the WB. **b.** Pressure plot at the engine expected location.

The next step is the computation of the WBE test case with the engine in the reference position but with no jet. Wing pressure distributions according to Figure 5 have been evaluated in Figure 6. A clear effect of the engine installation on the wing's pressure distribution can be observed. The shock front moves towards the leading edge of the wing in the region where the engine is placed. Furthermore, the shock becomes significantly weaker, as desired. The implementation of the engine produces an obvious difference in the value of the overall drag coefficient and on the resulting angle of attack at target lift coefficient, Figure 6. Due to the installation of the engine, an increase in drag by around 18% can be observed. The resulting angle of attack of the aircraft in cruise condition has to be increased from 2.41° for the WB to 3.73° for the WBE configuration.

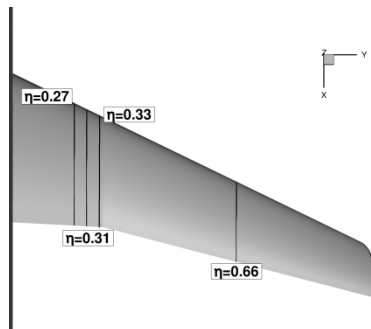


Fig. 5. Cuts for the pressure diagrams for different wing sections.

When an operational engine with inlet and jet effects is considered, the shock moves further upstream and becomes even weaker while the overall shape of the pressure distribution remains unchanged, see Figure 6. The inlet and jet effects influence the pressure field in all four evaluated sections.

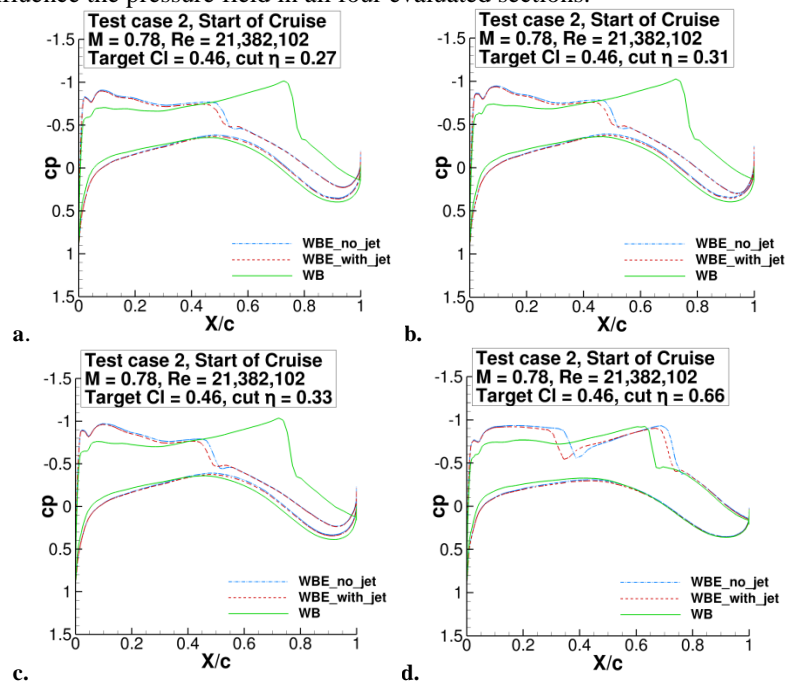


Fig. 6. Pressure diagrams for four cuts on the wing. Comparison between WB, WBE with no jet influence and WBE with jet (engine in reference position).

Therefore, the immediate consequence of the engine installation over the wing, even without the jet effect, is an upstream movement of the shock front by around 22.5% of the chord length. For pressure sections at $\eta = 0.27$, 0.31 and 0.33 a reduction of the shock strength is observed. The jet does not have an impact on the

basic slope of the pressure distribution, but it impacts the position of the shock in the inboard part of the wing with the shock becoming weaker. Nevertheless, the significant effects can be attributed to the engine installation itself and not to the presence of the jet or the inlet massflow. For the outboard cut at $\eta = 0.66$, the flow is strongly impacted by the engine and jet installation and a double shock front is identified. The reason for the double shock is a compensation of the lift losses due to the engine installation at the inboard part of the wing by an increase in angle of attack for the WBE configuration. Figure 7 presents a view on the isobars for both configurations.

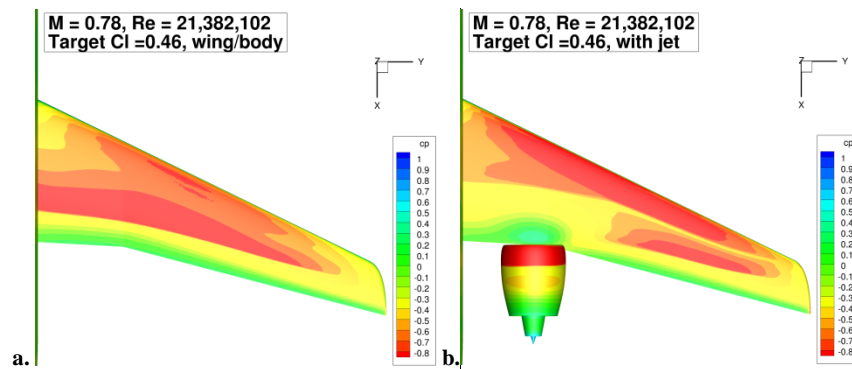


Fig. 7. Isobars on the WB (a.) and WBE (engine reference position) with jet on (b.).

The vertical position variations of the engine have not revealed significant changes with respect to the REF3 configuration with the engine at Z_{ref} . A comparison between the pressure distributions for the three different positions of the engine at the four wing cuts is depicted in Figure 8. The pressure distributions are widely unaffected up to about 60% local chord. The aft region of the suction side exhibits a strong impact of the engine installation. The shock on the upper surface moves slightly upstream when the engine is moved closer to the wing and even more upstream when the engine is placed further from the wing surface in the region where the engine is installed. At the station $\eta = 0.66$ larger differences can be seen due to the engine positioning. Yet, it has to be taken into account that for the present drag-focused study, the angle of attack is adapted to achieve the same C_L for all position variations. Therefore the aerodynamic background of the observed effects is yet to be fully investigated.

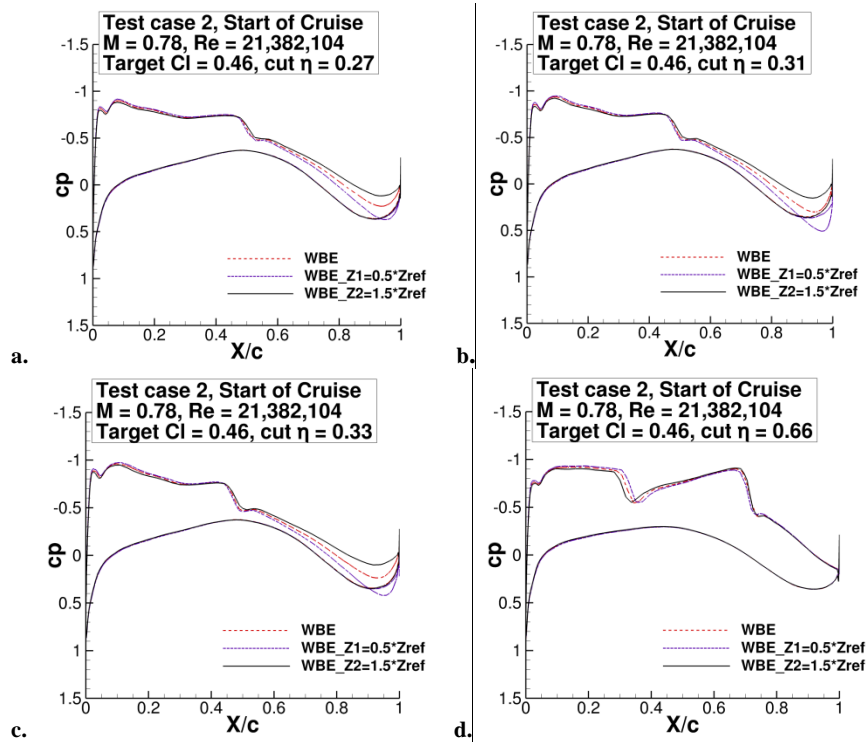


Fig. 8. Comparison of pressure plots for four cuts on the wing for the position variations.

Figure 9 depicts the Mach contours in the flow field for the WBE with the engine in the reference position (a) and WBE with the engine at Z_2 (b) for a cut through the engine middle plane.

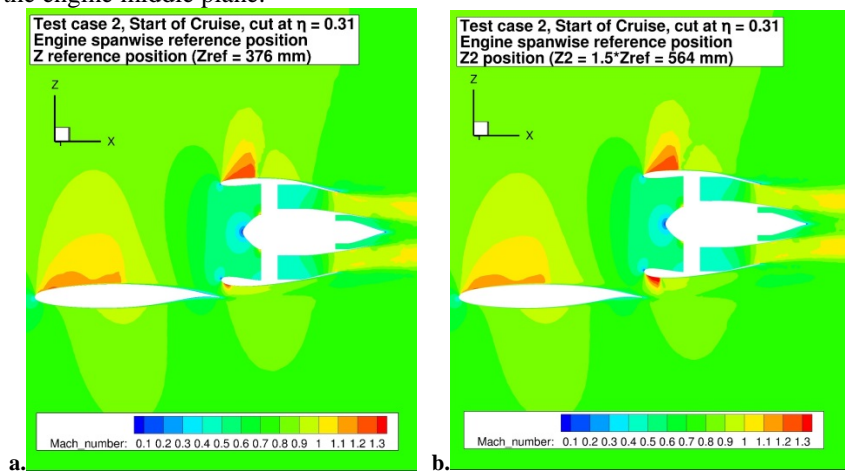


Fig. 9. Mach contour in the flow field for engine in the reference position (a) and engine at Z_2 (b)

Figure 9b shows the benefits of this engine position in terms of interactions between the flow on the wing and slower flow at the engine inlet. The flow is accelerating between wing rear part and engine lower lip. This is beneficial also in the reduction of a trailing edge separation (observed for the WB and the WBE with the engine closer to the wing's surface) in the region where the engine is installed.

Preliminary drag considerations

The evaluation of the interference drag is a crucial point in the study of OWM engines configurations and it is a complex task still in progress. The methodology planned to be adopted is described in [4]. Three components have to be calculated in order to assess the performance impacts of the different vertical positions of the engine in terms of interference drag.

- $\Delta C_{Dairframe}$, given by the forces acting on the wing/body portion of the WBE configuration minus the ones acting on the isolated wing/body;
- $\Delta C_{Dnacelle}$, given by the forces acting on the engine portion of the installed configuration minus the ones acting on the isolated nacelle. More specifically:

$$\Delta C_{Dnacelle} = C_{D,engine}(WBE)|_{C_L} - C_{PT,engine}(WBE)|_{C_L} - C_{D,engine}(E)|_{\alpha} + C_{PT,engine}(E)|_{\alpha}$$
The propulsive thrust coefficient C_{PT} of the engine must be taken into account. Therefore it is necessary to distinguish the aerodynamic surfaces from the propulsion surfaces.
- ΔC_{all} , given by the sum of the previous two.

Therefore, the values of the drag coefficients for the different aircraft components directly derived from the simulations cannot be used for a proper interference drag evaluation. In particular, the fan inlet force evaluation has to be done by a thrust/drag bookkeeping to differentiate between drag and thrust forces. Therefore the present evaluation intends to be a first estimation of the trends of the performance impact of the different positions of the engine on the airframe interference drag, assuming a constant inlet contribution. The airframe interference drag for the WBE with the engine at Z_{ref} has been taken as a reference.

Vertical engine position	$\Delta C_{Dairframe}/\Delta C_{Dairframe,Zref}$
Z_{ref}	1
Z_1	+2.64
Z_2	-0.94

Table 2. Airframe interference drag for the different engine positions

Neglecting the inlet forces, significant changes in the trends can be seen: for Z_1 a reduction in the airframe part of the interference drag is found. A thrust-drag analysis considering the inlet contribution as well as a decomposition of drag into physical components is scheduled for the near future.

5 Conclusions

A preliminary assessment of the potential of over-the-wing nacelle installations has been provided using a CFD approach solving RANS equations. The results for different configurations were compared in terms of isobars on the aircraft surface and pressure distributions. In addition to the known benefits in the reduction of acoustic noise and ground clearance, the study indicates that OWM nacelles have a potential with respect to the aerodynamic efficiency by properly balancing the inboard and outboard flowfield. Their implementation can provide a positive interference drag effect resulting in a more efficient configuration with respect to conventional UWM engine installations. However, their installation remains a challenging task which cannot be decoupled from a shape optimization process of the wing, the nacelle and the pylon. The pylon, in fact, is expected to have a strong influence on the resulting flow characteristics, for its large size due to the need of housing the main landing gear. The pylon design and the shape optimization of its junction to the wing and to the engine are therefore expected to have an impact on the choice of the optimum engine position. The cruise-efficient engine position will have to be assessed in the low speed regime, to ensure the feasibility of UHBR OW-installations also in take-off and landing conditions in conjunction with a circulation control system to allow short take-off and landing capabilities.

Acknowledgements

The authors like to acknowledge the funding of the present study by DFG as part of the Sonderforschungsbereich 880 "Grundlagen des Hochauftriebs künftiger Verkehrsflugzeuge" and Arno Ronzheimer from the Transport Aircraft Department of DLR for his valuable support.

References

1. Airbus S.A.S.: Flying by numbers, Global Market Forecast 2015-2034, p.9, Blagnac, France (2015)
2. L. Müller, W. Heinze, D. Kozulovic, M. Hepperle, R. Radespiel: Aerodynamic Installation Effects of an Over-the-Wing propeller on a High-Lift Configuration, *Journal of Aircraft*, Vol.51, No.1, p.249 (2014)
3. W. Heinze, T. Weiss: Main Data Sheet. A/C Type: SFB880 Reference Aircraft REF3-2015 (June 2015)
4. J.R. Hooker, A. Wick, C. Zeune, A. Agelastos: Over Wing Nacelle Installations for Improved Energy Efficiency, 31st AIAA Applied Aerodynamics Conference, San Diego, CA (June 2013)
5. CentaurSoft Homepage: <http://www.centaursoft.com>
6. J. Blazek: *Computational Fluid Dynamics: Principles and Applications*, ELSEVIER (2001)
7. TAU-Code User Guide, Release 2015.1.0 (May 2015)
8. T. Weiss, W. Heinze: Multidisciplinary design of a CESTOL aircraft with powered lift system, from *Fundamentals of High-Lift for Future Commercial Aircraft*, R. Radespiel, R. Semaan, Biennial Report, Braunschweig (2013)